On the computation of seismic energy in inelastic structures

André Filiatrault, Pierre Léger and René Tinawi

Department of Civil Engineering, Ecole Polytechnique de Montreal, P.O. Box 6079 Station A, Montreal, Canada, H3C 3A7

(Received March 1993; revised version accepted August 1993)

The explicit computation of energy balance for structures subjected to seismic excitation is useful to assess the accuracy with which dynamic equilibrium is achieved in each time-step. Examples on the use of the energy balance concept are presented in the first part of this paper for simple inelastic structures excited by various ground motions. It is shown how the energy approach can guide the designer in appreciating the nonlinear behaviour of the structure, the hierarchy of mechanisms that occur in time, and the ductility requirements of the various components. This was achieved using an unconditionally stable time marching algorithm with no algorithmic damping. A parametric study is then presented on the influence of algorithmic damping on seismic energy response of multi-degree-of-freedom structures. Finally, the Newmark-Beta method, with and without algorithmic damping, and the Alpha method are used in comparative analyses to evaluate the response of bilinear hysteresis models of multi-degree-of-freedom structures.

Keywords: algorithmic damping, earthquake, energy, seismic response

It is considered that a structure can survive a major earthquake if its structural energy absorption capacity is greater than the seismic input energy[1,2]. Therefore, most structures are designed to develop inelastic action, in critical components, that control the amount of stored seismic energy in the systems. The seismic input energy imparted to a structure is equal to the sum of the kinetic energy, the elastic strain energy, the energy dissipated by hysteretic action of the structural elements, and the energy dissipated by other nonyielding mechanisms (usually represented by viscous damping). The seismic energy dissipation and related damaged models of single-degree-of-freedom (SDOF) and multi-degrees-of-freedom (MDOF) systems have been studied by many researchers[3–7]. Moreover, energy balance computations have been used extensively in structural dynamics to assess the global performance of numerical integration procedures[8–14].

Very important work on the evaluation of the seismic energy in structures has been carried out recently by Uang and Bertero[15,16]. They have shown the influence of different earthquake ground motions and structural characteristics on the seismic input energy. In particular, the destructive potential of different earthquake records was assessed by comparing their energy spectra. The energy spectrum has the advantage of indirectly considering the effect of the duration of the earthquake. This parameter is not accounted for by the conventional response spectrum technique.

0141-0296/94/060425–12

Other formulations based on the use of energy in earthquake engineering have been proposed by several authors. Zahrah and Hall[7] considered energy absorption in linear and nonlinear SDOF systems subjected to earthquake excitations. Allahabadi and Powell[20] included energy computation in the DRAIN-2DX code. Schiff and Hall[17] and Tso *et al.*[18] used a modified version of the DRAIN-2D code[19] to evaluate seismic energy dissipation in low-rise steel frames and reinforced concrete frames, respectively. Hart and Wilson[8] implemented energy balance computations in the WAVES program to evaluate the earthquake energy balance in soil profiles. Filiatrault and Cherry[21,22] proposed an energy criterion for selecting the optimum properties of friction damped structures subjected to strong earthquakes. Aiken and Kelly[23] carried out shake table tests on nine-storey moment resisting steel frames using different types of energy absorbers as well as concentrically braced configurations. In this case the energy distribution throughout the various systems was obtained experimentally.

Energy computations have also been studied in other fields of structural dynamics[10–14]. In these studies, the energy balance check was obtained from the difference between the external energy, computed from external applied loads, and the kinetic and internal energies computed from internal resisting forces. Maximum errors in energy balance should not exceed 2% to 5% to ensure numerical stability and accuracy of the response of inelastic

systems subjected to blast and concentrated transient loads[14,24].

With the development of personal computers and workstations, nonlinear time-step earthquake analyses incorporating energy balance computations are becoming more available for design offices. Although this increase in analytical sophistication is thought to be beneficial, it also raises some concerns about the interpretation and use of the results. So far, investigations using energy balance computations in inelastic earthquake response analysis have been almost exclusively based on the Newmark average acceleration method[28] that exhibits no algorithmic damping, thus preserving the input energy as long as the time step remains constant[9,17,25,26]. However, algorithmic damping becomes necessary to control the higher modes of MDOF structures which are often not representative of the behaviour of the system because of the distortions introduced by the selection of a finite number of DOF[27]. Algorithmic damping may also be necessary when the time-step retained for a practical analysis may be too large to integrate accurately the high frequency content of the response.

Although it would be unwise to damp out the response of higher modes in gradually decaying ductile systems, such as frames, the situation is very different for brittle continuous systems, such as unreinforced concrete dams in which cracking occurs[34,36]. In these latter systems, the higher modes could be distorted due to the lack of mesh refinement. In such cases, algorithmic damping can be advantageous, provided the response is controlled by the lower modes. For example, the introduction of algorithmic damping with the Alpha method was found necessary to control spurious deformation mechanisms of cracked elements where the global stability of the solution procedure was controlled by energy balance[36].

Numerical dissipation to damp out the spurious participation of higher modes can be introduced in the Newmark method by modification of the integration parameters. However, algorithmic damping can only be obtained at the expense of reduced accuracy (from second- to first-order). The introduction of an additional parameter, α (alpha), to control the dissipation properties of Newmark's method was proposed by Hilber *et al.*[29]. With an appropriate choice of parameters, the Alpha method retains second-order accuracy and provides an effective dissipation of high-frequency components of the response[28].

This paper discusses the use of the energy balance concept to appreciate the inelastic structural behaviour and to assess the accuracy of nonlinear earthquake analyses. In the first part of the paper, the energy balance equation for a general nonlinear MDOF system, subjected to earthquake excitation, is derived from the equilibrium equations. The implementation of this equation in a computer code is discussed.

Examples on the use of the energy balance concept are then presented in the second part of the paper for simple inelastic structures excited by various ground motions. For this purpose, Newmark's method, based on the classical constant-average acceleration method ($\beta = \frac{1}{4}$) is used. This algorithm has the advantage of being unconditionally stable for linear systems and produces, for small time-steps, accurate solutions not affected by algorithmic damping. The results show how the energy approach can guide the designer in appreciating the nonlinear behaviour of the structure, the hierarchy of mechanisms that occur in time, and the ductility requirements of the various components.

Finally, in the third part of the paper, the seismic energy response of MDOF structures is investigated for the Newmark method, with and without algorithmic damping, and for the Alpha method. Bilinear hysteresis models of simple MDOF shear buildings with different strength levels are considered in parametric analyses where the time steps are systematically varied.

Energy balance for nonlinear multidegree-of-freedom systems

Derivation

The governing differential equations of motion to be solved for a general nonlinear MDOF system undergoing a rigid base translation from an earthquake ground motion are given by

$$[M]\{\ddot{u}(t)\} + [C]\{\dot{u}(t)\} + \{F_r(t)\} = -[M]\{r\}\ddot{x}_g(t) + \{F_s\} \tag{1}$$

where $[M]$ is the global mass matrix; $[C]$ is the global viscous damping matrix which accounts for all supplemental energy dissipation mechanisms other than inelastic hysteretic behaviour of the structural members; $\{u(t)\}$, $\{\dot{u}(t)\}$ and $\{\ddot{u}(t)\}$ are the global displacement, velocity, and acceleration vectors, respectively, relative to the moving base at time t; $\{F_r(t)\}$ is the global nonlinear restoring force vector at time t, generated by the hysteretic properties of the structural elements; $\{r\}$ is a vector coupling the direction of the ground motion input with the direction of the displacement DOF; $\ddot{x}_g(t)$ is the ground acceleration at time t; and $\{F_s\}$ is the global preseismic static load vector. In the case of multiple support excitation, the right-hand side of equation (1) needs to be modified accordingly[34].

To transform equation (1) into an energy balance equation, it is first premultiplied by the transpose of the relative velocity vector, $\{\dot{u}(t)\}^T$, and each term is integrated over the time domain.

$$\int \{\dot{u}(t)\}^T[M]\{\ddot{u}(t)\}\mathrm{d}t + \int \{\dot{u}(t)\}^T[C]\{\dot{u}(t)\}\mathrm{d}t + \int \{\dot{u}(t)\}^T\{F_r(t)\}\,\mathrm{d}t = -\int \{\dot{u}(t)\}^T[M]\{r\}\ddot{x}_g(t)\,\mathrm{d}t + \int \{\dot{u}(t)\}^T\{F_s\}\,\mathrm{d}t \tag{2}$$

Using the differential relationships between displacement, velocity and acceleration, the time variable can be replaced in equation (2) in favour of displacement and velocity variables.

$$\int \{\dot{u}(t)\}^T[M]\{\mathrm{d}\dot{u}(t)\} + \int \{\dot{u}(t)\}^T[C]\{\mathrm{d}u(t)\} + \int \{\mathrm{d}u(t)\}^T\{F_r(t)\} = -\int \{\mathrm{d}u(t)\}^T[M]\{r\}\ddot{x}_g(t) + \int \{\mathrm{d}u(t)\}^T\{F_s\} \tag{3}$$

The first term of equation (3) can be integrated to yield an explicit energy balance equation for the system.

$$T_r(t) + D(t) + R(t) = I_r(t) + S(t) \tag{4}$$

where

$$T_r(t) = \frac{1}{2}\{\dot{u}(t)\}^T[M]\{\dot{u}(t)\}$$

$$D(t) = \int \{\dot{u}(t)\}^T[C]\{du(t)\}$$

$$R(t) = \int \{du(t)\}^T\{F_r(t)\}$$

$$I_r(t) = -\int \{du(t)\}^T[M]\{r\}\ddot{x}_g(t)$$

$$S(t) = \int \{du(t)\}^T\{F_s\} \tag{5}$$

Physically the components of equation (4) have the following meaning:

$T_r(t)$	relative kinetic energy of system at time t
$D(t)$	energy dissipated by viscous damping at time t
$R(t)$	energy absorbed at time t as result of deformations of structural elements
$I_r(t)$	relative seismic input energy at time t
$S(t)$	work done by preseismic applied loads

The term $R(t)$ can be divided into two components

$$R(t) = U(t) + H(t) \tag{6}$$

where $U(t)$ is the recoverable elastic strain energy, and $H(t)$ is the energy dissipated by the hysteretic behaviour of the structural elements. Expressions for $U(t)$ and $H(t)$ depend on the assumed hysteresis models. For example, if a bilinear action–deformation hysteresis model is selected, as illustrated in *Figure 1*, the following explicit expressions can be used

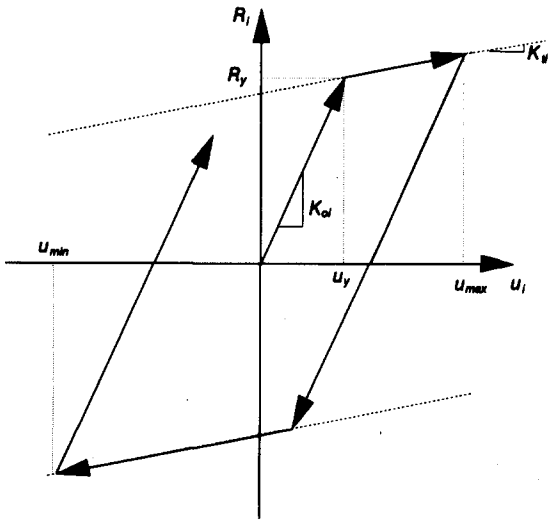

Figure 1 Bilinear hysteretic model

$$U(t) = \frac{1}{2}\sum_i \frac{R_i^2(t)}{K_{oi}}$$

$$H(t) = H(t - \Delta t) + \sum_i \left[R_i(t - \Delta t) + \frac{1}{2}(u_i(t) - u_i(t - \Delta t))K_{ti}\right] - \frac{1}{2}\sum_i \left[\frac{R_i^2(t) - R_i^2(t - \Delta t)}{K_{oi}}\right] \tag{7}$$

The relative seismic input energy to the system is equal to the inertia forces integrated through their relative displacements. It is very important to realize that the input energy depends on the characteristics of the earthquake ground motion and also on the dynamic properties of the structure.

Relative and absolute seismic input energy

The energy balance equation derived above is based on equivalent lateral seismic forces applied to a rigid base structure. This approach eliminates consideration of the rigid body translation of the structure and, for this reason, is called a 'relative' formulation. The rigid body translation of the structure can be included explicitly in an 'absolute' energy formulation. Although several authors have derived the absolute formulation directly from equation (2)[7,15–18,25], it provides insight to obtain it from the relative energy balance equation. To achieve this, integration by parts of the first right-hand-side term in equation (2) is performed.

$$I_r(t) = -\{\dot{u}(t)\}^T[M]\{r\}\dot{x}_g(t) + \int \{\ddot{u}(t)\}^T[M]\{r\}\dot{x}_g\, dt \tag{8}$$

The relative acceleration vector $\{\ddot{u}(t)\}$ can be expressed in terms of the absolute acceleration vector $\{\ddot{u}_a(t)\}$ such that

$$\{\ddot{u}(t)\} = \{\ddot{u}_a(t)\} - \{r\}\ddot{x}_g(t) \tag{9}$$

Substituting equation (9) into equation (8) yields

$$I_r(t) = -\{\dot{u}(t)\}^T[M]\{r\}\dot{x}_g(t) + \int \{\ddot{u}_a(t)\}^T[M]\{r\}\dot{x}_g\, dt - \int \ddot{x}_g(t)\{r\}^T[M]\{r\}\dot{x}_g\, dt \tag{10}$$

Using the differential relationships between the ground displacement, velocity and acceleration, equation (10) can be written as

$$I_r(t) = -\{\dot{u}(t)\}^T[M]\{r\}\dot{x}_g(t) + \int \{\ddot{u}_a(t)\}^T[M]\{r\}\, dx_g(t) - \int \dot{x}_g(t)\{r\}^T[M]\{r\}\, d\dot{x}_g(t) \tag{11}$$

Integrating the last term of equation (11) yields

$$I_r(t) = -\{\dot{u}(t)\}^T[M]\{r\}\dot{x}_g(t) + \int \{\ddot{u}_a(t)\}^T[M]\{r\}\, dx_g(t) - \frac{1}{2}\dot{x}_g(t)\{r\}^T[M]\{r\}\dot{x}_g(t) \tag{12}$$

Substituting this new expression for the relative energy input into equation (4) leads to

$$\frac{1}{2}\{\dot{u}(t)\}^T[M]\{\dot{u}(t)\} + \{\dot{u}(t)\}^T[M]\{r\}\dot{x}_g(t) + \frac{1}{2}\dot{x}_g(t)\{r\}^T[M]\{r\}\dot{x}_g(t) + D(t) + H(t) = \int\{\ddot{u}_a(t)\}[M]\{r\}\,dx_g(t) + S(t) \quad (13)$$

The first three terms of this equation can be combined such that

$$\frac{1}{2}\{\{\dot{u}(t) + \{r\}\dot{x}_g(t)\}^T[M]\{\{\dot{u}(t) + \{r\}\dot{x}_g(t)\} + D(t) + H(t) = \int\{\ddot{u}_a(t)\}[M]\{r\}\,dx_g(t) + S(t) \quad (14)$$

But from equation (9) we have

$$\{\dot{u}(t)\} + \{r\}\dot{x}_g(t) = \{\dot{u}_a(t)\} \quad (15)$$

Substituting equation (15) into (14) leads to an absolute energy balance equation

$$T_a(t) + D(t) + H(t) = I_a(t) + S(t) \quad (16)$$

where

$$T_a(t) = \frac{1}{2}\{\dot{u}_a(t)\}^T[M]\{\dot{u}_a(t)\}$$

$$I_a(t) = \int\{\ddot{u}_a(t)\}^T[M]\{r\}\,dx_g(t) \quad (17)$$

Physically the components of equation (17) have the following meaning: $T_a(t)$ equals the absolute kinetic energy of the system at time t; and $I_a(t)$ equals the absolute seismic input energy at time t.

The absolute input energy to the system is equal to the base shear integrated through the absolute ground displacement. Both energy formulations, relative and absolute, are mathematically equivalent. As was pointed out by Uang and Bertero[15,16], the real physical input energy is explicitly considered by the absolute energy formulation. The relative formulation, however, has the advantage of only introducing the ground acceleration in the calculations. The absolute formulation requires both ground displacement and acceleration. Both energy formulations produce similar results[15] for the practical range of structural periods from 0.1 s to 5.0 s.

Discrete energy expressions

The kinetic energy at a given time t can be obtained directly from the instantaneous relative velocity vector $\{\dot{u}(t)\}$. All the other energy quantities, however, need integration through the time domain. For practical implementation of the energy formulation in a computer code, numerical integrations are required. Many schemes are available to carry out these integrations. Using the trapezoidal rule, for example, the continuous energy expressions can be implemented in a computer code using the following discrete energy expressions.

$$D(t) = D(t-\Delta t) + \frac{1}{2}(\{\dot{u}(t-\Delta t)\} + \{\dot{u}(t)\})^T[C]\,(\{u(t)\} - \{u(t-\Delta t)\})$$

$$H(t) = H(t-\Delta t) + \frac{1}{2}(\{u(t)\} - \{u(t-\Delta t)\})^T\,(\{F_r(t-\Delta t)\} + \{F_r(t)\})$$

$$I_r(t) = I_r(t-\Delta t) - \frac{1}{2}(\{u(t)\} - \{u(t-\Delta t)\})^T[M]\{r\}\,(\ddot{x}_g(t-\Delta t) + \ddot{x}_g(t))$$

$$I_a(t) = I_a(t-\Delta t) + \frac{1}{2}(\{\ddot{u}_a(t)\} - \{\ddot{u}_a(t-\Delta t)\})^T[M]\{r\}\,(x_g(t-\Delta t) + x_g(t))$$

$$S(t) = S(t-\Delta t) + (\{u(t)\} - \{u(t-\Delta t)\})^T\{F_s\} \quad (18)$$

Alternatively, the elastic strain and hysteretic energies can be computed by closed form expressions such as in equation (7).

Using energy balance as a criterion for accuracy

Since the energy terms in equations (4) and (16) can be computed individually as the time-marching integration progresses, the energy balance error, $EBE(t)$, can be calculated at each time-step and used as a criterion for indicating the global accuracy achieved by a given algorithm. The energy balance error can be normalized in percent as follows

$$EBE_r(t) = \frac{|I_r(t) + S(t) - T_r(t) - D(t) - H(t)|}{|I_r(t)|} \times 100\% \quad (19)$$

for a relative energy formulation, and

$$EBE_a(t) = \frac{|I_a(t) + S(t) - T_a(t) - D(t) - H(t)|}{|I_a(t)|} \times 100\% \quad (20)$$

for an absolute energy formulation.

In a computer code, a tolerance limit can be set on the energy balance error, which stops the computations or automatically reduce the time-step, if exceeded. This procedure can save time and computer costs if too large a time-step is used in an initial trial run. As discussed earlier, a tolerance of 2% to 5% has been suggested for practical analyses[14,24].

Newmark's and Alpha methods

Only the Newmark and Alpha methods are considered in this study. Other integration schemes are difficult to control with regard to algorithmic damping. The Wilson-θ method, for example, suffers from overshoot problems under certain initial conditions[35]. Also, this method provides unreasonably high values of algorithmic damping.

The Newmark algorithm for numerical integration of equation (1) is defined by

$$[\tilde{k}(t)]\{\Delta u(t)\} = \{\Delta \tilde{P}(t)\} \tag{21}$$

with

$$[\tilde{k}(t)] = [k(t)] + \frac{1}{\beta \Delta t^2}[M] + \frac{\gamma}{\beta \Delta t}[C]$$

$$\{\Delta \tilde{P}(t)\} = -[M]\{r\}\Delta \ddot{x}_g(t) + [M]\left(\frac{1}{\beta \Delta t}\{\dot{u}(t)\} + \frac{1}{2\beta}\{\ddot{u}(t)\}\right) + [C]\left(\frac{\gamma}{\beta}\{\dot{u}(t)\} + \left(\frac{\gamma}{2\beta} - 1\right)\Delta t\{\ddot{u}(t)\}\right) \tag{22}$$

where $[k(t)]$ is the tangent stiffness matrix at time t

$$\{\Delta \dot{u}(t)\} = \frac{\gamma}{\beta \Delta t}\{\Delta u(t)\} - \frac{\gamma}{\beta}\{\dot{u}(t)\} - \frac{\gamma \Delta t}{2\beta}\{\ddot{u}(t)\} - \left(\frac{\gamma}{2\beta} - 1\right)\Delta t\{\ddot{u}(t)\} \tag{23}$$

$$\{\ddot{u}(t + \Delta t)\} = [M]^{-1}(-[M]\{r\}\ddot{x}_g(t + \Delta t) + \{F_s\} - [C]\{\dot{u}(t + \Delta t)\} - \{F_r(t + \Delta t)\}) \tag{24}$$

When $\gamma = \frac{1}{2}$, the method is second-order accurate and exhibits no algorithmic damping. If $\gamma > \frac{1}{2}$, algorithmic damping is introduced and the accuracy reduces to the first order. Taking $\beta = (\gamma + \frac{1}{2})^2$ maximizes the high frequency dissipation for a given value of $\gamma > \frac{1}{2}$[30]. For the time-step to period ratio, $\Delta t/T < 0.5$, viscous damping controls the low-frequency dissipation and is ineffective to control high-frequency dissipation which is controlled by algorithmic damping[30]. Viscous damping and algorithmic damping are thus not additive for $\Delta t/T < 0.5$. Hilber *et al.*[29] introduced the parameter α in Newmark's method to improve its performance when algorithmic damping is required. Equation (24) is replaced by

$$[M]\{\ddot{u}(t + \Delta t)\} + [C]\{\dot{u}(t + \Delta t)\} + (1 + \alpha)[k(t + \Delta t]\{u(t + \Delta t)\} - \alpha[k(t)]\{u(t)\} = -[M]\{r\}\ddot{x}_g(t + \Delta t) + \{F_s\} \tag{25}$$

Equation (25), used in this study, corresponds to the original form of the Alpha method as proposed by Hilber *et al.*[29]. The Alpha method was later extended to apply the α parameter to the damping matrix as well[30]. If the parameters are selected such that $-\frac{1}{3} \leq \alpha \leq 0$, $\gamma = (1 - 2\alpha)/2$, and $\beta = (1 - \alpha)^2/4$ the method is second-order accurate. With $\alpha = 0$ there is no algorithmic damping, as α decreases there is an increase in algorithmic damping for elastic systems as shown in *Figure 2*.

Examples of energy computation

To appreciate the use of the energy balance concept in nonlinear earthquake analyses, various numerical examples are presented for an ensemble of two-storey framed structures idealized as nonlinear (elasto-plastic) 2-DOF systems. Even for these simple structural models, the energy balance approach reveals the structural responses in a different perspective, which could help to better understand the nonlinear behaviour of these structures.

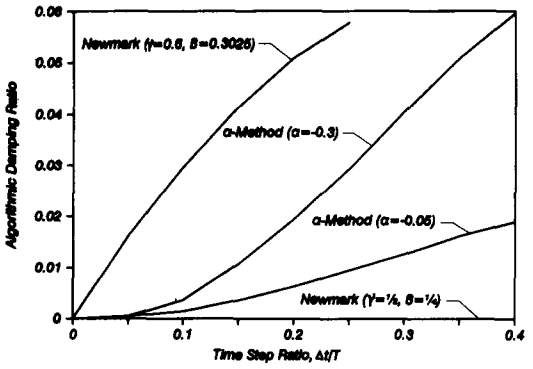

Figure 2 Algorithmic damping ratios for α-methods and Newmark method (adapted from Hughes[28])

Structural models and assumptions

The basic structural models used in the analyses consist of four different two-storey steel plane frames as shown in *Figure 3*. Four structural systems are included: a moment resisting frame (MRF); a braced frame (BF); a soft storey frame (SSF) obtained by removing the first-floor braces from the braced frame (BF); and finally a base isolated frame (BIF) obtained by 'retrofitting' the braced frame (BF) with lead–rubber hysteretic bearing.

The MRF and BF were designed as ductile frames for a peak acceleration of 0.20 g according to the National Building Code of Canada[31]. The tension–compression braces of the BF were chosen on the basis of the seismic detailing requirements of the Canadian Steel Code[32]. These requirements ensure stable energy dissipation in the braces while all the other members remain elastic.

Only one DOF per floor was considered in the analyses except the BIF, where one DOF was prescribed just above the bearings and a second one at the top floor. The resulting structural properties are presented in *Table 1*. The lateral shear–drift relationship for each floor was modelled as an elastic-perfectly plastic hysteretic behaviour. Rayleigh-type viscous damping, with 2% critical damping in each mode of vibration based on the elastic system, was considered for each structure.

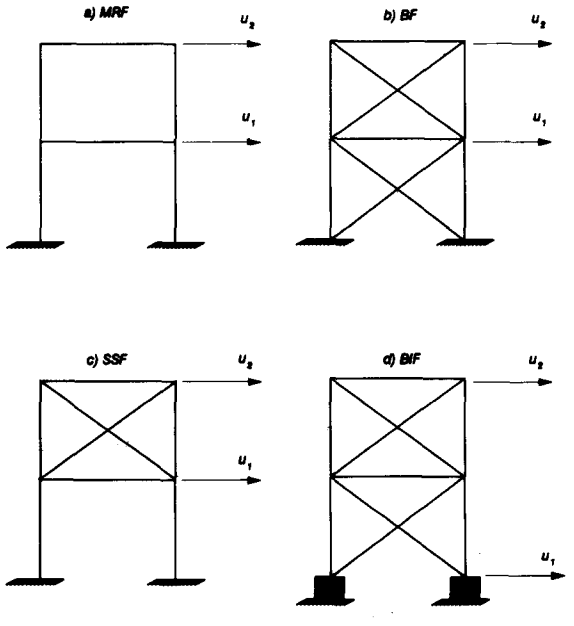

Figure 3 2-DOF structural models

Table 1 Properties of 2-DOF structural models

Frame	Mass (kN-s²/m) Level 1	Mass (kN-s²/m) Level 2	Stiffness (kN/m) Level 1	Stiffness (kN/m) Level 2	Yield force (kN) Level 1	Yield force (kN) Level 2	Period (s) Mode 1	Period (s) Mode 2
MRF	50	50	6850	5500	390	320	0.89	0.36
BF	100	100	169000	169000	2630	2630	0.25	0.09
SSF	100	100	6850	169000	390	2630	1.08	0.11
BIF*	100	100	169000	169000	2630	2630	2.02	0.13

* Bearing stiffness = 1960 kN/m
Viscous damping = 2% critical in each mode

The base isolators were modelled as elastic springs with total lateral stiffness, K_i, based on earlier experimental and analytical studies[33,37–40] and expressed by the following empirical formula

$$K_i = W \tag{26}$$

where W is the total weight of the structure in kN and K_i represents the postelastic shear stiffness of the bearings and is expressed in kN m^{-1}.

For simplicity, the energy dissipation of the isolators was neglected. This assumption is justified since the hysteresis loops of typical lead–rubber isolators are quite narrow with modest energy dissipation capabilities[33].

Choice of earthquake ground motions

The four structural configurations were subjected to three different ground motions and their seismic responses were compared from an energy point of view. As shown in *Figure 4*, the earthquake records considered were

- 1988 Saguenay earthquake (Chicoutimi (Quebec), LONG)
- 1940 El Centro earthquake (S00E)
- 1977 Romania earthquake (Bucharest, N-S)

All the records were scaled to a peak ground acceleration of 0.5 g and only the first 15 s of each record were considered. The absolute acceleration response spectra of these three scaled seismic events are shown in *Figure 5* for their complete duration. The Saguenay record represents an earthquake with an energy content associated with short periods, the El Centro earthquake has its energy distributed over a fairly broad period band, while the Romanian earthquake is an example of a seismic event with an energy content concentrated at the high end of the period spectrum.

Choice of time-step algorithm

Since the purpose of the analyses is to obtain the energy distribution in simple nonlinear systems, accurate solutions not affected by numerical damping are sought. For this purpose, the Newmark-Beta average acceleration method, with no algorithmic damping ($\gamma = \frac{1}{2}$ and $\beta = \frac{1}{4}$), was chosen as the algorithm to integrate the equations of motion. The results presented are based on a time-step increment of 0.001 s which ensured virtually no energy balance error in all analyses.

Comparison of energy time-histories

The energy time-histories, based on the relative formulation (see equation (4)), are presented in *Figures 6–9* for the four structural systems subjected to the three earthquake ground motions considered.

Although the energy time-histories generated from a

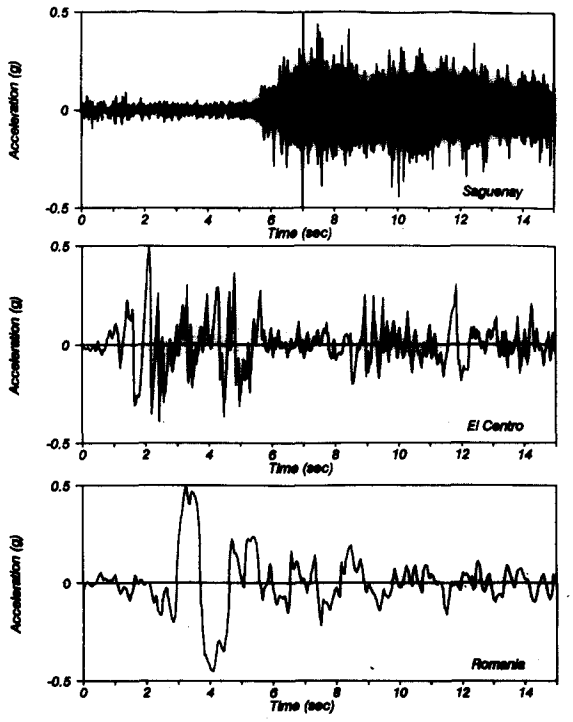

Figure 4 Accelerograms of earthquake ground motions scaled to 0.5 g

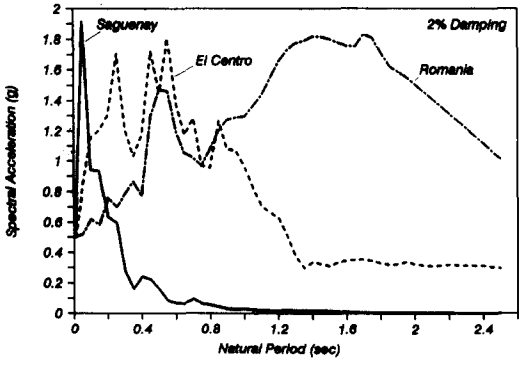

Figure 5 Absolute acceleration response spectra

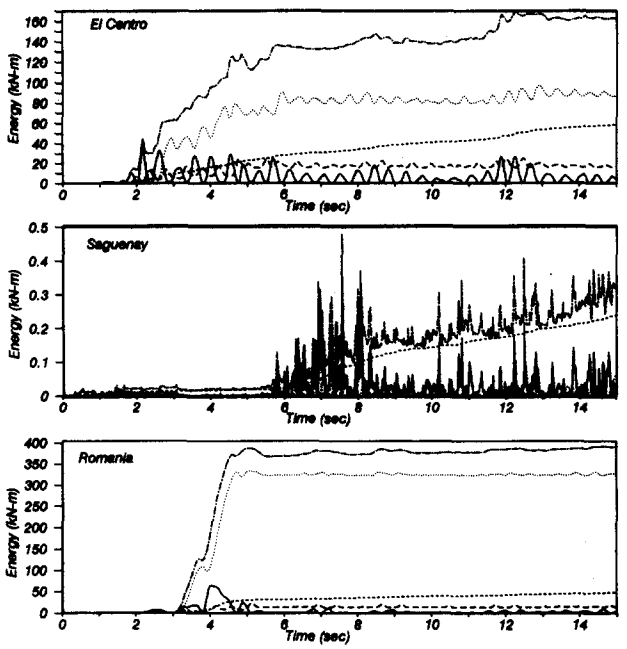

Figure 6 Energy time-histories for MRF. ——— Relative kinetic energy ------ Energy dissipated by viscous damping ····· First floor absorbed energy --- Second floor absorbed energy -·-·-·- Relative energy input

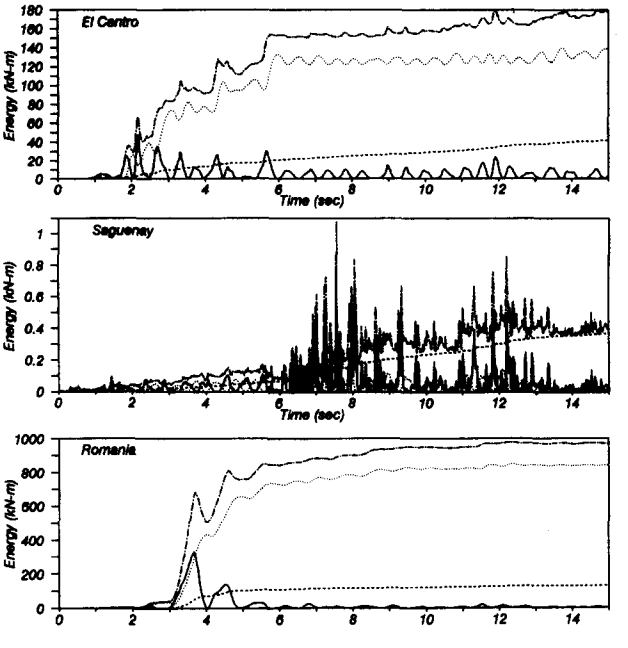

Figure 8 Energy time-histories for SSF. ——— Relative kinetic energy ------ Energy dissipated by viscous damping ····· First floor absorbed energy --- Second floor absorbed energy -·-·-·- Relative energy input

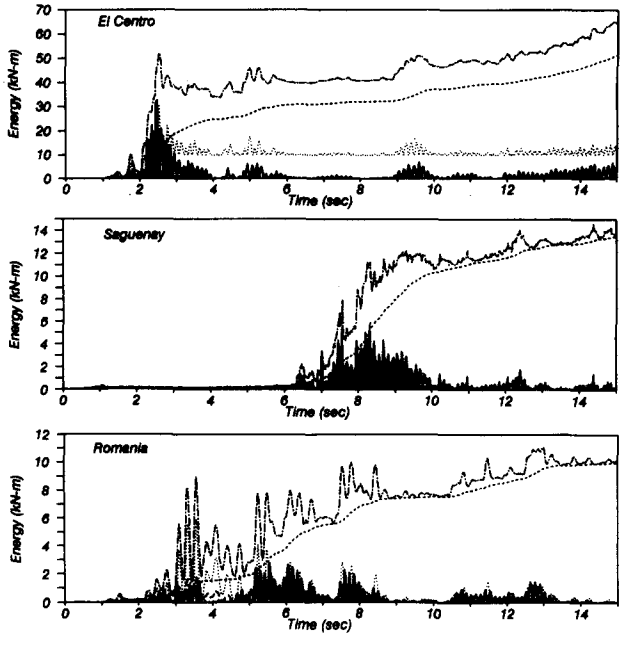

Figure 7 Energy time-histories for BF. ——— Relative kinetic energy ------ Energy dissipated by viscous damping ····· First floor absorbed energy --- Second floor absorbed energy -·-·-·- Relative energy input

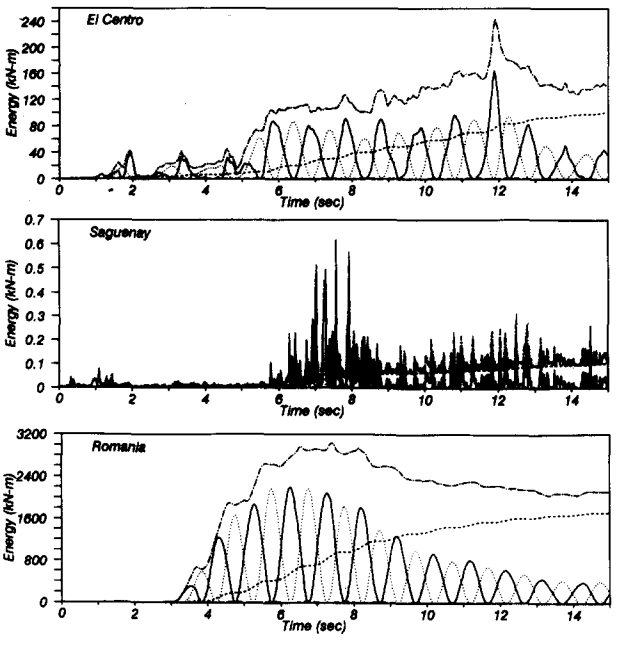

Figure 9 Energy time-histories for BIF. ——— Relative kinetic energy ------ Energy dissipated by viscous damping ····· First floor absorbed energy --- Second floor absorbed energy -·-·-·- Relative energy input

given record vary widely from one structural system to the other, each energy component exhibits a particular pattern. The kinetic energy oscillates from zero, when the structure reaches local maximum deflections, to positive peaks when the structure passes through its initial undeformed position. The energy dissipated by viscous damping always increases with time. As expected, the absorbed energies of the first and second floors present two distinct components: a recoverable elastic component, represented by oscillations out of phase from the kinetic energy, and a nonrecoverable component represented by sudden shifts towards positive values as yielding occurs in time. The seismic input energy generally increases with time, but local valleys occur as some of the energy returns into the foundation when the equivalent seismic forces are in the opposite direction of the relative displacements.

The most striking observation that can be made from the results presented in *Figures 6–9* is that, although the earthquake records have all the same duration and peak acceleration, there are very large amplitude differences (up to four

orders of magnitude) between the various energy time-histories for a given structure. To better appreciate this wide difference in the energy quantities, *Figure 10* presents, using the same scale, the relative seismic input energy time-histories for the different earthquake records and structural models. The BIF is very efficient in practically eliminating the seismic input energy for the El Centro and Saguenay records. For the Romania earthquake, however, the situation is completely reversed. The largest values of the seismic input energy occur in the BIF under the Romania record. For this earthquake, retrofitting the BF with base isolators would be detrimental because of the quasiresonance phenomenon occurring due to the close proximity of the fundamental period of the BIF to the predominant period of the ground motion (see *Table 1* and *Figure 5*). The maximum seismic energy transmitted to the BIF by the Romania earthquake is approximately 250 times larger than the energy transmitted to the original BF by the same record.

The consequences, from an energy perspective, of introducing a soft storey in the first floor of the original BF can be seen in *Figure 11* for the El Centro and Romania records. For the Romania record, the maximum hysteretic energy demand in the first floor of the SSF is 170 times larger than the hysteretic energy in the first floor of the original BF. The corresponding figure for the El Centro record is about 4.5 times.

Effect of algorithmic damping on energy balance

A reference solution using Newmark's average acceleration method ($\gamma = \frac{1}{2}$, $\beta = \frac{1}{4}$), that does not introduce algorithmic damping, is used as a basis to evaluate the performance of dissipative integration methods. The difference in $EBE(t)$ among various integration methods using the same time step, Δt, and iterative solution strategy, can be attributed mainly to algorithmic damping but period elongation, and the order of accuracy of the method may also have an influence.

Systems analysed

Three different moment resisting frames idealized as shear buildings with 3, 10, and 25 DOF were designed according to the National Building Code of Canada[31] for a peak ground acceleration of 0.26 g.

In the code, the total minimum lateral seismic force, that is used with a load factor of 1, is given by

$$V = \frac{V_e}{R} U \tag{27}$$

where V_e is the equivalent lateral force at the base of the structure representing the elastic response, R is the force modification factor representing the available ductility in well detailed structures, and U is a calibration factor rep-

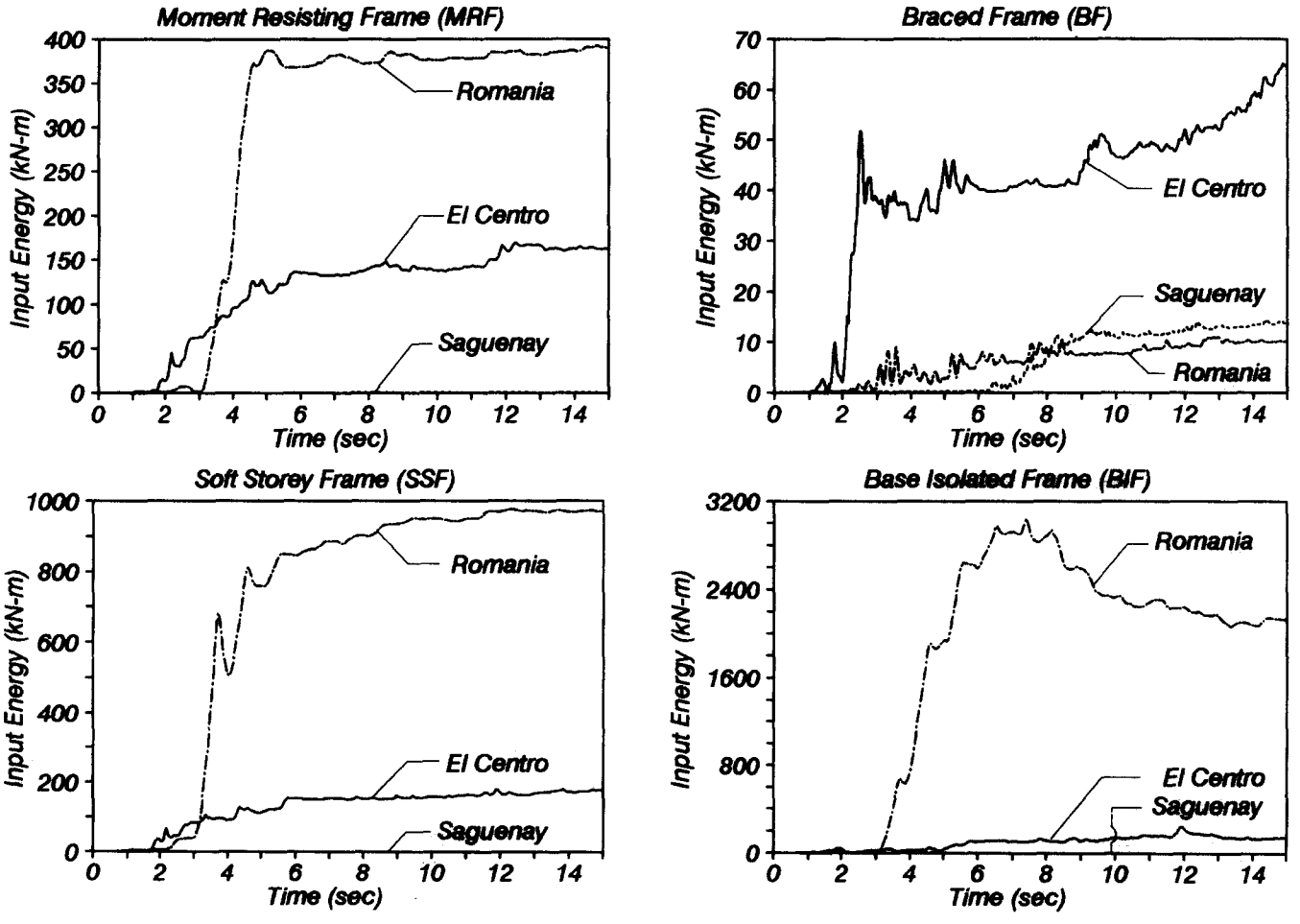

Figure 10 Relative seismic input energy time-histories

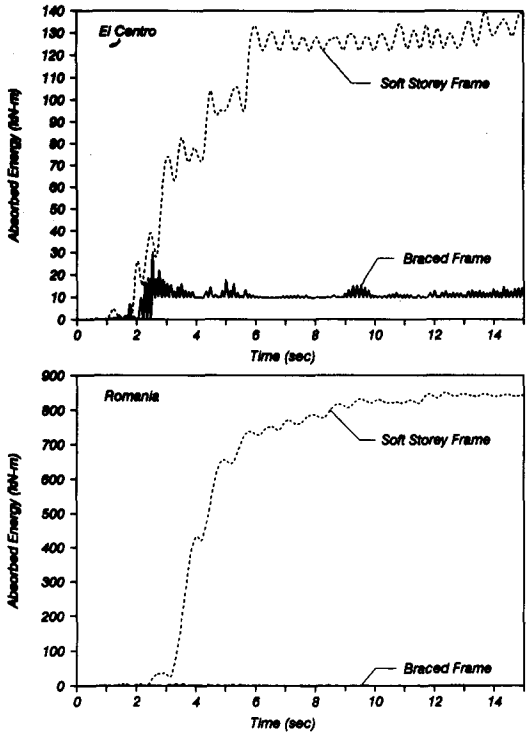

Figure 11 First floor elastic strain + hysteretic energy time-histories

resenting the desired level of protection based on experience. The value of R ranges from 1, for nonductile structural systems expected to remain elastic under the design earthquake ground motion, to 4 for ductile moment resisting frames with good seismic detailing. For SDOF structures, the value of R is directly related to the displacement ductility demand of the system.

The systems properties, summarized in *Tables 2* and *3*, are calibrated such that the fundamental period of vibration,

Table 2 Properties of shear buildings analysed

Level*	Elastic stiffness K_o (kN m^{-1})	Yield force**, R_y (kN)
3 DOF		
1	274000	540
2	205000	450
3	137000	270
10 DOF		
1–2	248000	957
3–4	201500	908
5–6	155000	795
7–8	108500	617
9–10	62000	374
25 DOF		
1	232000	1513
2–4	220400	1509
5–7	197200	1474
8–10	174000	1405
11–13	150800	1301
14–16	127600	1163
17–19	104400	991
20–22	81200	783
23–25	58000	541

* Each level has a mass of 100 kN-s^2 m^{-1}
** R_y is given for $R=4$, $2R_y$ corresponds to $R=2$

Table 3 Free-vibration properties of shear beam buildings analysed

Mode	Period, T (s)	$\Delta t/T$*	% Modal mass
3 DOF			
1	0.300	0.067	85.2
2	0.120	0.167	96.3
3	0.079	0.255	100.0
10 DOF			
1	1.000	0.020	76.2
2	0.400	0.050	89.1
3	0.247	0.081	94.0
4	0.177	0.113	96.4
5	0.149	0.135	97.2
6	0.124	0.161	98.5
7	0.108	0.185	99.0
8	0.093	0.216	99.4
9	0.081	0.247	99.7
10	0.070	0.284	100.0
25 DOF			
1	2.500	0.008	75.9
2	0.957	0.021	87.9
3	0.585	0.034	92.4
4	0.422	0.047	94.7
5	0.330	0.061	96.1
6	0.271	0.074	97.0
7	0.230	0.087	97.6
8	0.204	0.098	98.0
9	0.182	0.110	98.4
10	0.165	0.121	98.6
11	0.151	0.133	98.8
12	0.142	0.141	98.9
13	0.134	0.149	99.7
14	0.125	0.160	99.3
15	0.118	0.169	99.4
16	0.113	0.177	99.5
17	0.106	0.189	99.6
18	0.102	0.197	99.6
19	0.095	0.209	99.7
20	0.092	0.218	99.7
21	0.086	0.231	99.8
22	0.082	0.243	99.9
23	0.078	0.255	99.9
24	0.074	0.270	99.9
25	0.069	0.288	100.0

* for $\Delta t = 0.02$ s

T_1, of each structure corresponds to the code value of $0.1N$, where N is the number of storeys (DOF) of the structure. The first 20 s of the S00E component of the 1940 El Centro earthquake, scaled by a factor of 0.95 to approximate the code elastic design spectra, are used as input motion. Rayleigh damping based on initial elastic properties using 5% critical in the first mode and the mode required to obtain 95% effective modal mass is used in all analyses. The equations of motion are solved by the Newton–Raphson method using equilibrium iterations.

The integration procedures based on the Newmark method (NM), and the Alpha method (AM) which have been used in parametric analyses where the time-step was systematically varied are listed in *Table 4*.

The first method is the classical, first-order accuracy, constant-average acceleration method which is unconditionally stable and does not generate any algorithmic damping. The second procedure is of second-order accuracy ($\gamma > 0.5$) and maximizes the high frequency dissipation[28] with $\beta = (\gamma + \frac{1}{2})^2$. The third scheme is also of second-order accuracy ($\gamma = (1 - 2\alpha)/2$ and $\beta = (1 - \alpha)^2/4$)

Table 4 Numerical integration procedures considered (NM Newmark's method; AM Alpha method)

No	Method	α	β	γ	Characteristics
1	NM	0	$\frac{1}{4}$	$\frac{1}{2}$	No algorithmic damping
2	NM	0	0.3025	0.6	Algorithmic damping
3	AM	−0.3	0.3025	0.6	Algorithmic damping
4	AM	−0.3	0.4225	0.8	Very high algorithmic damping

but offers better control of the algorithmic damping for lower modes ($\alpha = -0.3$ instead of 0)[28]. Finally, the last procedure in *Table 4* introduces very high algorithmic damping and is considered for comparison purposes.

Seismic energy responses

Figure 12 shows the time histories of the roof displacement, the input seismic energy, and the energy dissipated for the 25-storey building analysed by the Newmark methods with a time-step increment of 0.02 s. The use of the integrator with algorithmic damping produces very small changes in the roof displacement and input energy responses. The hysteretic and damping energy are slightly reduced. These results, although related to algorithmic damping, are consistent with the findings of Zahrah and Hall[7]. They have observed that viscous damping has little effect on the amount of energy imparted to a structure by an earthquake, and that damping may have more influence on the amount of hysteretic energy producing damage. The integrator with algorithmic damping produces an error in energy balance of approximately 5% at the end of the earthquake. This means 5% of the input energy has been artificially dissipated by the algorithmic damping mechanism in the analysis.

Influence of the time-step and force reduction factor

Figure 13 shows the influence of the time step and severity of the inelastic response on the amount of input energy dissipated by algorithmic damping. Three cases are considered for the 25-DOF building, (i) linear elastic; (ii) moderately inelastic ($R = 2$); and (iii) strongly inelastic ($R = 4$). The NM($\beta = 0.25$, $\gamma = 0.5$) provides the reference where no error in energy balance is observed due to algorithmic damping. The $EBE_a(t)$ (virtually identical to $EBE_r(t)$ in all analyses) at the end of the earthquake ($t = 20$ s), which corresponds to the effect of energy dissipation by algorithmic damping, has been reported in the figures. The dissipative effect of the other methods decrease rapidly with a reduction in time-step. The effectiveness of algorithmic damping to dissipate a fraction of the input energy is reduced as the system is going to respond more strongly in the inelastic range. For example, the linear system dissipates almost twice as much energy by algorithmic damping than the strongly inelastic system ($R = 4$). As the system becomes inelastic there is a softening of the stiffness that produces an elongation of the instantaneous period of vibration $T_i(t)$. For a constant Δt value, there is a reduction of the ratio $\Delta t/T_i(t)$ decreasing the effectiveness of algorithmic damping (see *Figure 2*). Since for the 25-DOF structure the global response is strongly dominated by the lower modes, there are very small differences between the NM ($\alpha = 0$, $\beta = 0.3025$, $\gamma = 0.6$) and the AM ($\alpha = -0.3$, $\beta = 0.3025$, $\gamma = 0.6$) responses.

Influence of the fundamental period of vibration

Figure 14 shows the influence of a reduction in the fundamental period of the structure on the EBE_a values at the end of the earthquake. As the fundamental period is reduced, the effectiveness of algorithmic damping increases. Larger EBE_a values can thus be observed for the three-storey building. Furthermore, since 'higher' modes

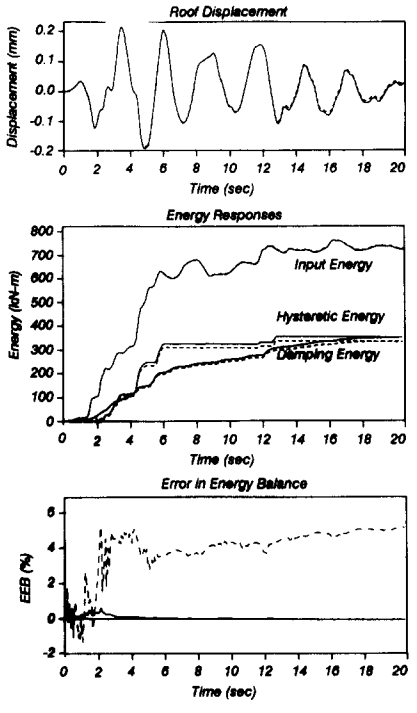

Figure 12 Time-histories of seismic response of 25-storey building, $R = 4$, $\zeta = 5\%$ ——— NM ($\alpha = 0$, $\beta = 0.25$, $\gamma = 0.5$) ------ NM ($\alpha = 0$, $\beta = 0.3025$, $\gamma = 0.6$)

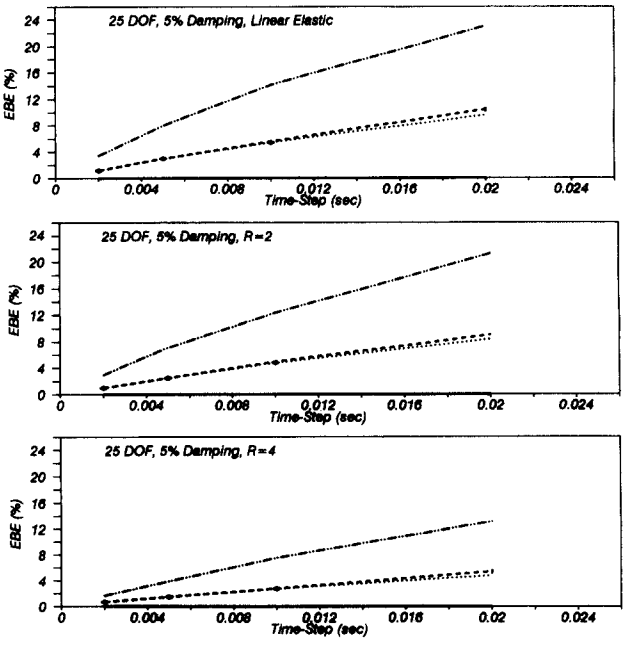

Figure 13 Influence of time-step and structural nonlinearity on energy dissipated by algorithmic damping ——— NM ($\alpha = 0$, $\beta = 0.25$, $\gamma = 0.5$) ------ NM ($\alpha = 0$, $\beta = 0.3025$, $\gamma = 0.6$) ····· AM ($\alpha = -0.3$, $\beta = 0.3025$, $\gamma = 0.6$) —·—·— AM ($\alpha = -0.3$, $\beta = 0.4225$, $\gamma = 0.8$)

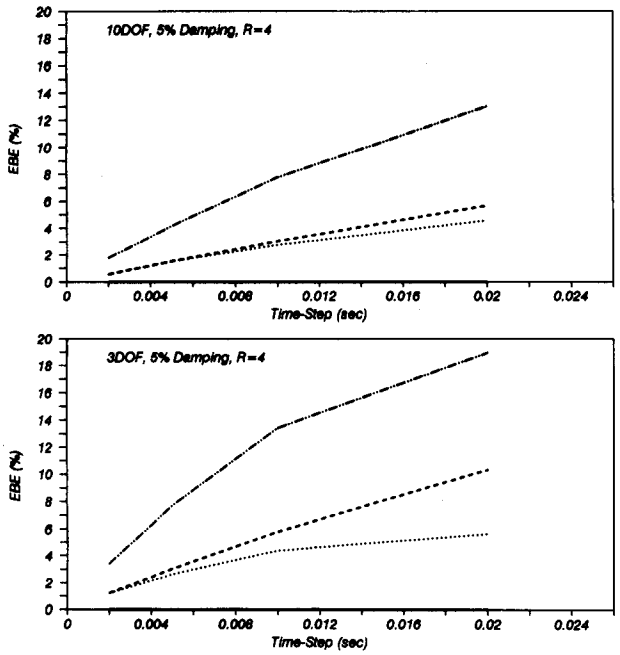

Figure 14 Influence of fundamental structural period on energy dissipated by algorithmic damping ——— NM ($\alpha = 0$, $\beta = 0.25$, $\gamma = 0.5$) ------ NM ($\alpha = 0$, $\beta = 0.3025$, $\gamma = 0.6$) ····· AM ($\alpha = -0.3$, $\beta = 0.3025$, $\gamma = 0.6$) ·—·—· AM ($\alpha = -0.3$, $\beta = 0.4225$, $\gamma = 0.8$)

are more important for the three-storey building that the other structures, there are wider differences among the NM ($\alpha = 0$, $\beta = 0.3025$, $\gamma = 0.6$) and the AM ($\alpha = -0.3$, $\beta = 0.3025$, $\gamma = 0.6$) responses for $\Delta t > 0.01$ s.

Figure 15 shows that the ratio $|H(t = 20\text{ s})/I(t = 20\text{ s})|$, which can be interpreted as a damage index[16,25,26] is slightly reduced by algorithmic damping. If the AM ($\alpha = -0.3$, $\beta = 0.4225$, $\gamma = 0.8$) is excluded, a maximum reduction of the order of 10% is observed for the three-storey building analysed with $\Delta t = 0.02$ s.

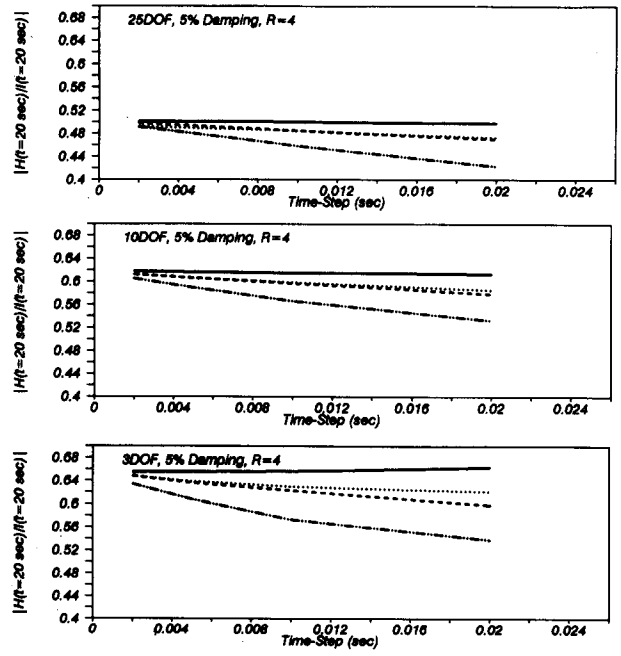

Figure 15 Influence of algorithmic damping on damage index $|H(t = 20\text{ s})/I(t = 20\text{ s})|$ ——— NM ($\alpha = 0$, $\beta = 0.25$, $\gamma = 0.5$) ------ NM ($\alpha = 0$, $\beta = 0.3025$, $\gamma = 0.6$) ····· AM ($\alpha = -0.3$, $\beta = 0.3025$, $\gamma = 0.6$) ·—·—· AM ($\alpha = -0.3$, $\beta = 0.4225$, $\gamma = 0.8$)

Conclusions

The use of the energy balance formulation in a nonlinear earthquake analysis program is a rational and appealing procedure, requiring little extra computational effort, to assess the accuracy of the numerical results. The implementation of such an energy procedure allows the evaluation of the global accuracy of a single run without having to perform a second analysis for comparison. Also, a tolerance limit can be set on the energy balance error, which stops the computations or automatically reduces the time-step if exceeded and thereby saves time and engineering effort.

The most positive aspect of the energy balance approach lies in the evaluation of the dissipated energy of the various structural components. This approach could be particularly useful in retrofitting existing structures, where most of the input energy should be directed to the added structural (or mechanical) dissipative components.

A virtually exact energy balance can be achieved using the Newmark average acceleration method ($\gamma = 0.5$, $\beta = 0.25$), that does not exhibit algorithmic damping, with relatively large time-step ($\Delta t = 0.02$ s). However, it might be desirable in some analyses to use an integration method that provides numerical dissipation to damp out the spurious participation of higher modes that are not representative of the real behaviour of the structures. In this case, a quasi-exact energy balance cannot be obtained unless a very small time-step, that annihilates the algorithmic damping, is used. It thus become important to understand how the energy responses of the systems are affected by algorithmic damping.

Acknowledgments

The authors wish to thank S. Dussault for his assistance in performing some of the computer analyses presented in this paper. The support of the Natural Sciences and Engineering Research Council of Canada, which provided operating grants in support of this project, is also gratefully acknowledged.

References

1 Kuwamura H. and Galambos, T. V. 'Earthquake loads for structural reliability', *J. Struct. Engng, ASCE* 1989, **115**, 2166–2183
2 Housner, G. W. and Jennings, P. C. 'The capacity of extreme earthquake motions to damage structures'. *Structural and geotechnical mechanics*, W. J. Hall (Ed.) Prentice-Hall, Englewoods Cliffs, NJ, 1977 pp 102–116
3 Fajfar, P. and Krawinkler, H. (Eds) *Nonlinear seismic analysis and design of reinforced concrete buildings* Elsevier Applied Sciences, London, 1992
4 Fajfar, P., Vidic, T. and Fischinger, M. 'A measure of earthquake motion capacity to damage medium-period structures', *Soil Dyn. Earthquake Engng* 1990, **9**, 236–242
5 McCabe, S. L. and Hall, W. J. 'Assessment of seismic structural damage', *J. Struct. Engng, ASME* 1989 **115**, 2166–2183
6 Tembulkar, J. M. and Nau, J. M. 'Inelastic modelling and seismic energy dissipation', *J. Struct. Engng, ASCE* 1987, **113**, 1373–1377
7 Zahrah, T. F. and Hall, W. J. 'Earthquake energy absorption in SDOF structures', *J. Struct. Engng, ASCE* 1984, **110** (8), 1757–1772
8 Hart, J. D. and Wilson, E. L. 'Simplified earthquake analysis of buildings including site effects'. Rep. UCB/SEMM-89/23, University of California, 1989
9 Filiatrault, A., Tinawi, R. and Léger, P. 'The use of energy balance in nonlinear seismic analysis'. *Proc. 10th World Conf. on Earthquake Engng*, Madrid, Spain, Vol. 7, pp 4111–4116
10 Belytschko, T. and Schoeberle, D. F. 'On the unconditional stability of an implicit algorithm for nonlinear structural dynamics', *J. Appl. Mech., ASME* 1975, **42**, 865–869

11 Hughes, T. J. R. 'Stability, convergence and growth and decay of energy of the average acceleration method in nonlinear structural dynamics', *Comput. Struct.* 1976, **6**, 313–324

12 Hughes, T. J. R. 'A note on the stability of Newmark's algorithms in nonlinear structural dynamics', *Int. J. Num. Meth. Engng* 1977, **11**, 383–386

13 Vu-Quoc, L. and Olsson, M. 'New predictor/corrector algorithms with improved energy balance for a recent formulation of dynamic vehicule/structure interaction', *Int. J. Num. Meth. Engng* 1991, **23**, 223–253

14 Beshara, F. B. A. and Virdi, K. S. 'Nonlinear finite element dynamic analysis of two-dimensional concrete structures', *Comput. Struct.* 1991, **41**, 1281–1294

15 Uang, C.-M. and Bertero, V.V. 'Evaluation of seismic energy in structures', *Earthquake Engng Struct. Dyn.* 1990, **19**, 77–90

16 Bertero, V.V. and Uang, C.-M. 'Issues and future directions in the use of an energy approach for seismic-resistant design of structures'. In *Nonlinear seismic analysis and design of reinforced concrete buildings*, P. Fajfar and H. Krawinkler (Eds), Elsevier Applied Science, London, 1992, pp 95–104

17 Schiff, S. D., Hall, W. J. and Foutch, D. D. 'Seismic performance of low-rise steel perimeter frames', *J. Struct. Engng, ASCE* 1991, **117** (ST2), 546–562

18 Tso, W. K., Zhu, T. J. and Heidebrecht, H. C. 'Seismic energy demands on reinforced concrete moment-resisting frames', *Earthquake Engng Struct. Dyn.* 1993, **22** (5), 533–545

19 Kannan, A. E. and Powell, G. H. 'DRAIN-2D, a general purpose computer program for dynamic analysis of inelastic plane structures'. Rep. EERC 73-6, Earthquake Engineering Research Center, University of California, Berkeley, CA, 1973

20 Allahabadi, R. and Powell, G. H. 'DRAIN-2DX user guide'. Rep. UCB/EERC-88-06, Earthquake Engineering Research Center, University of California, Berkeley, CA, 1988

21 Filiatrault, A. and Cherry, S. 'Comparative performance of friction damped systems and base isolation systems for earthquake retrofit and aseismic design', *Earthquake Engng Struct. Dyn.* 1988, **16** (3), 389–416

22 Filiatrault, A. and Cherry, S. 'Seismic design spectra for friction damped structures', *J Struct. Engng, ASCE* 1990, **16** (ST5), 1334–1355

23 Aiken, I. D. and Kelly, J. M. 'Earthquake simulator testing and analytical studies of two energy-absorbing systems for multistorey structures'. Rep. UCB/EERC-90/03, Earthquake Engineering Research Center, University of California, Berkeley, CA, 1990

24 Belytschoko, T., Chiapetta, R. L. and Bartel, H. D. 'Efficient large scale nonlinear transient analysis by finite elements', *Int. J. Num. Meth. Engng* 1976, **10**, 579–596

25 Léger, P. and Dussault, S. 'Seismic energy dissipation in MDOF structures', *J. Struct. Engng, ASCE* 1992, **118**, 1251–1269

26 Léger, P. and Dussault, S. 'Nonlinear seismic response analysis using vector superposition methods', *Earthquake Engng Struct. Dyn.* 1992, **21**, 163–176

27 Wakefield, R. R., Nazmy, A. S. and Billington, D. P. 'Analysis of seismic failure in skew RC bridge', *J. Struct. Engng, ASCE* 1991, **117**, 972–986

28 Hughes, T. J. R., *The finite element method, linear static and dynamic finite element analysis*, Prentice-Hall, Englewood Cliffs, NJ, 1987

29 Hilber, H. M., Hughes, T. J. R. and Taylor, R. L. 'Improved numerical dissipation for time integration algorithms in structural dynamics', *Earthquake Engng Struct. Dyn.* 1977, **5**, 283–292

30 Hohberg, J.-M. 'A joint element for the nonlinear dynamic analysis of arch dams'. *PhD thesis*, Swiss Federal Institute of Technology, Zurich, Switzerland, 1992

31 National Building Code of Canada, Associate Committee on the National Building Code. National Research Council of Canada, Ottawa, Ontario, Canda, 1990

32 Canadian Standard Association 'Steel structures for buildings (limit state design)'. CAN3-S16.1-M89. National Standard of Canada, Rexdale, Ontario, Canada, 1989

33 Robinson, W. 'Lead-rubber hysteretic bearings suitable for protecting structures during earthquakes', *Earthquake Engng Struct. Dyn.* 1982, **10**, 593–600

34 Clough, R. and Penzien, J. *Dynamics of structures*, McGraw Hill, 1975

35 Hilber, H. M. 'Analysis and design of numerical integration methods in structural dynamics'. EERC Rep. 76-29, Earthquake Engineering Research Center, University of California, Berkeley, November 1986

36 Bhattacharjee, S. S. and Léger, P. 'Seismic cracking and energy dissipation in concrete gravity dams', *Earthquake Engng Struct. Dyn.* 1993, **22**, (to appear)

37 Lee, D. M. and Medland, I. C. 'Estimation of base isolated structure responses', *Bull. NZ Nat. Soc. Earthquake Engng* 1978, **11** (4), 234–244

38 Meggett, L. M. 'Analysis and design of a base-isolated reinforced concrete frame building', *Bull. NZ Nat. Soc. Earthquake Engng* 1978, **11** (4), 245–254

39 Blakeley, R. W. G., Cormack, L. G. and Stockwell, M. J. 'Mechanical energy dissipation devices', *Bull. NZ Nat. Soc. Earthquake Engng* 1978, **13** (3), 264–268

40 Eisenberger, M. and Rutenberg, A. 'Seismic base isolation of asymmetric shear buildings', *Engng Struct.* 1986, **8**, 2–8